The Ice Ages

by

John Reid

The Ice Ages

Introduction

The idea that the Earth was once much colder than at present has been debated by scientists since the early 18th century. In 1824, Danish-Norwegian geologist, Jens Esmark, appears to have been the first to propose that the Earth had undergone climatic changes and that these were caused by changes in the Earth's orbit. Serbian astrophysicist, Milutin Milankovitch, was the first to "put the numbers in" to Esmark's theory (Milankovitch, 1941), and these orbital variations are now known as "Milankovitch Cycles". In more recent times, Hays et al. (1976) used oxygen isotope ratios in ocean sediment cores to show that Esmark, Milankovitch (and many others) were correct in this proposal. Hays et al. conclude:

1. *Three indices of global climate have been monitored in the past 450,000 years in Southern Hemisphere ocean-floor sediments.*

2. *Over the frequency range* 10^{-4} *to* 10^{-5} *cycles per year, climatic variance of these records is concentrated in three spectral peaks at periods of 23,000, 42,000 and approximately 100,000 years. These peaks correspond to the dominant periods of the earth's solar orbit, and contain respectively about 10, 25 and 50 percent of the climatic variance.*

3. *The 42,000-year climatic component has the same period variations in the obliquity of the earth's axis and retains a constant phase relationship with it.*

4. *The 23,000-year portion of the variance displays the same periods (about 23,000 and 19,000 years) as the quasi-periodic precession index.*

5. *The dominant, 100,000-year climatic component has has an average period close to, and is in phase with, orbital eccentricity. Unlike the correlations between climate and the higher frequency orbital variations (which can be explained on the assumption that the climate system responds linearly to orbital forcing), an explanation of the correlation between climate and eccentricity probably requires and assumption of non-linearity.*

6. *It is concluded that changes in the earth's orbital geometry are the fundamental cause of the succession of Quaternary ice ages.*

7. *A model of future climate based on the observed orbital-climate relationships, but ignoring anthropogenic effects, predicts that the long-term trend over the next several thousand years is toward Northern Hemisphere glaciation.*

Since that paper was published, there have been numerous incremental improvements in pinning down the time scales of ocean sediment sequences. Most importantly isotope ratios in ice cores, which act as proxies for global temperature, have become available from Greenland and the Antarctic ice cap. These not only tally with the ocean sediment time series but, with one or two exceptions, support the above conclusions.

The 100,000-year spectral peak contains half the variance and certainly dominates graphs of the spectra unless they are plotted on logarithmic scales. Hays et al. were well aware that variations in the eccentricity of the earth's orbit were not sufficient to give rise to such a comparatively strong peak, which is why they appealed to an unknown non-linear mechanism to account for it. Their use of "approximately" indicates that they were also well aware that visual inspection of their data in the time domain reveals no 100,000-year cycle. Interstadials (i.e. interglacials)

are separated by 80,000 years or 120,000 years, multiples of the obliquity period. Others have noted these discrepancies, e.g. Maslin and Ridgwell (2005).

Here we show that this peak is not statistically significant. Its large size is due solely to the integrating effect of Fourier's heat equation which results in a power law temperature spectrum with an index of -2 as described by Fourier's heat equation.

It is also not the case that higher frequency variations "can be explained on the assumption that the climate system responds linearly to orbital forcing": the rapidity of ice age terminations compared with ice age onsets implies that some non-linear mechanism must be involved. Elsewhere in their paper, Hays et al. recognise this but still have difficulty accounting for the 100,000-year peak.

Orbital Parameters

Temperatures, T, derived from EPICA Dome C ice cores (Jouzel et al., 2007) covering the period from 490 kyr to the present were examined. For spectral analysis purposes it was desirable that time series be created comprising a sequence of values sampled at equal intervals of time. However, as a result of ice flow behaviour, more recent ice core strata from near the surface are sampled much more densely in time than are deeper, older strata. Time series were constructed by partitioning the data into sampling intervals of equal length. Values lying within each sampling interval were then averaged and the mean assigned to the mid-time of that sampling interval. The time interval was chosen as 1 kyr with 491 samples spanning the period from 490 kyr BP to the present.

Figure 1**a** shows 1 kyr averages of EPICA Dome C Ice Core Deuterium temperature estimates due to Jouzel et al. (2007). Figure 1**b** shows the first differences of the sequence shown in Figure 1**a**, ΔT. Its mean, m, and $\pm 2\sigma$ levels are shown as dashed lines. The temperature differences exceed the upper 2σ level during terminations when the temperature is rapidly increasing. Also shown are the secular variations in the Earth's orbital parameters derived from the data and the *MATLAB* programs originally due to Berger (1979) and Berger and Loutre (1991) and later used by Huybers (2006) and Huybers and Eisenman (2006). The vertical lines in these three figures represent the time at which the temperature differences of Figure 1**b** were more than 2σ above the mean, i.e. the times of terminations as defined here. On four out of five occasions in Figure 1**o**, terminations occurred at times of increasing obliquity, but the one near 250 kyr BP did not. On the other hand, in Figure 1**p** the three most recent terminations occurred at times of increasing precession, but the earliest two did not.

Figure 2 shows spectra in the form of periodograms of the five time series shown in Figure 1 with vertical scales displaced arbitrarily for ease of comparison.

Both the obliquity and precession spectra have multiple peaks. In this way they resemble the spectra of amplitude modulated (AM) and frequency modulated (FM) radio signals. Radio engineers refer to the largest peak as the "carrier" and the other peaks as "side-bands".

The spectrum of ΔT in Figure 2 is almost flat implying that the time series is unselfcorrelated. If we take as null hypothesis the hypothesis that the population time series of ΔT is indeed unselfcorrelated as discussed above then confidence limits can be placed on each ordinate value. The horizontal dashed lines in Figure 2 are the upper and lower 99.9% confidence limits for the ΔT spectrum (Reid, 2019).

It can be seen that the carrier peaks in the obliquity and precession spectra give rise to significant peaks in the ΔT spectrum at the 99.9% level. Peaks corresponding to the side-bands are not present. The statistical significance of the obliquity and precession peaks implies that the temperature time series does indeed have deterministic sinusoidal components: it is not purely

stochastic. On the other hand, the so-called "eccentricity peak" near $(f) = 10^{-2}$ is not significant and can be regarded as noise, as can other peaks in the ΔT spectrum at higher frequencies.

A mechanism for rapid terminations

Huybers (2006) has pointed out that while the intensity of summer insolation is primarily controlled by the .044 kyr^{-1} precession frequency, early Pleistocene glacial cycles occurred at the .0246 kyr^{-1} obliquity frequency because glaciers are sensitive to insolation integrated over the duration of the summer. Nevertheless this cannot be the whole story because, as can be seen in Figure 1, Termination III (∼250 kyr BP) occurred at a time of declining NH obliquity but increasing precession. Huybers pointed out that ice sheet ablation is only indirectly related to insolation via air temperature and will not occur when air temperature is below the freezing point of water. For this reason he proposed that insolation only be realistically considered as forcing at a given latitude when it exceeded a threshold sufficient to raise the air temperature above 0°C. Huybers proposed a threshold of 275 W/m^2 at 65°N. Introducing this threshold had the effect of bringing the precession cycle back into play so that ice sheet ablation was no longer dependent on the obliquity cycle alone. This led to an improved fit between glacial cycles and the Earth's orbital parameters.

However, this does not account for the remarkable rapidity of the terminations: ice sheets that took more than 40,000 years to form collapsed within 4,000 years or so as can be seen in Figures 1a and 1b. Quasi-sinusoidal orbital components, while related to temperature to some degree in both phase (Figure 1) and frequency, (Figure 2) gave rise to the saw-tooth temperature variations of Figure 1a. This requires some sort of positive feedback and a mechanism for storing heat or enthalpy from one summer to the next. Ablation by solar radiation and raised air temperatures alone does not provide such a mechanism. Furthermore, there is a need to account for the fact that terminations did not occur on every occasion when conditions were suitable. There is a random element: increased insolation only seems to increase the probability of ice sheet collapse rather than act as a fully deterministic cause.

Water is an atypical liquid in having its maximum density at 4.0°C – well above its freezing point. This implies that a body of water between 0°C and 4.0°C will behave much like a solar pond in that the upward convection of heat is suppressed. In solar ponds this condition is set up and maintained by adding salt to maintain the density gradient, but in melt ponds it happens naturally. In solar ponds incoming solar radiation heats most of the top 2 m. There is a surface 'mixed layer' due to wind induced turbulence, and below 2 m heat is preserved. The density gradient suppresses convection, and conduction is negligibly small – ∼1 W/m^2 compared with ∼100 W/m^2 from incoming radiation. In calm conditions the water heated to 4.0°C by radiation might be expected to sink to the bottom of the pond due to 'inverse convection'. To first order this will commence spontaneously when the Rayleigh number exceeds a critical value of 1700 for which the length scale is ∼5 metres. In summer, wind induced turbulence will predominate, and the melt lake will be well mixed to the bottom because density variations will be too small to induce stratification. In winter, a surface cover of ice will form rapidly allowing turbulence to die out and the water to become stratified. At depth the water will remain liquid because its latent heat cannot escape.

On sea ice, the warmed water finally thaws through to the base of the ice and mixes with the ocean beneath so that melt ponds on sea ice only last for a single season. In a melt pond over land, however, radiatively heated water will mix down and melt the ice beneath it until bedrock is reached. From then on extra heat will ablate the edges of the pond, and the pond will become larger. Each summer more heat will be added, and the pond will grow in area in proportion to

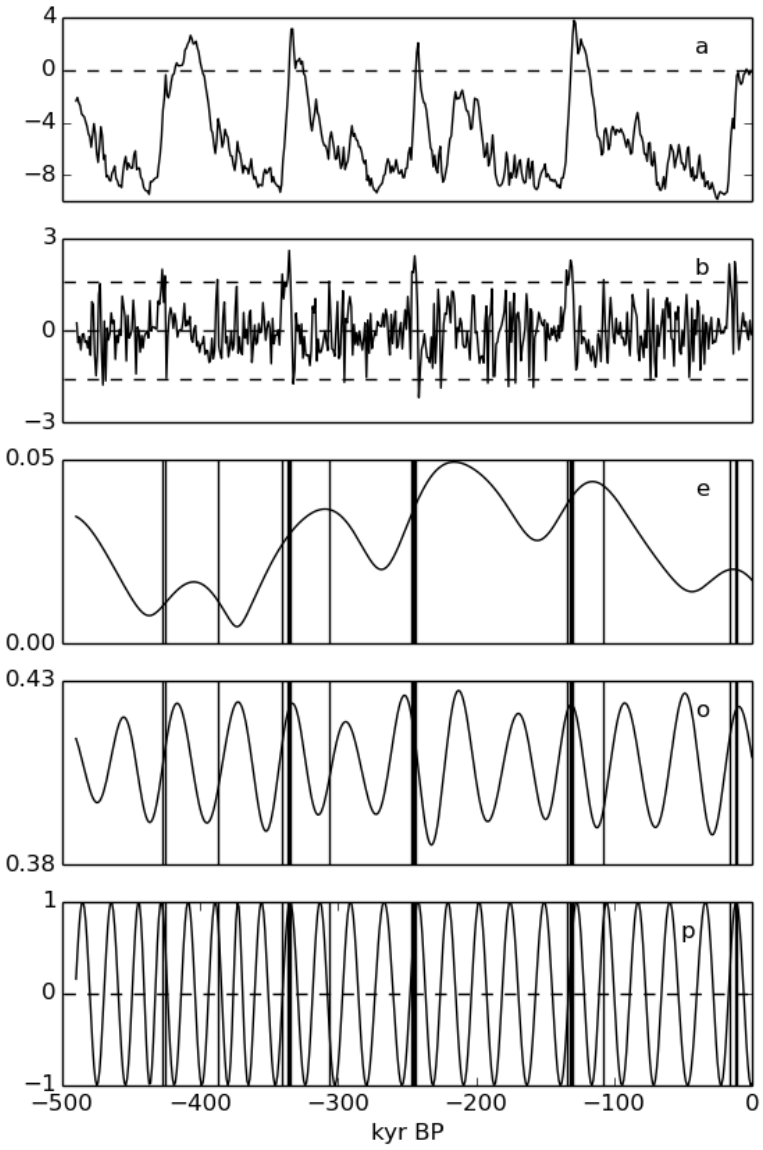

Figure 1: **a** 1 kyr averaged temperatures, T, derived from EPICA Dome C ice cores. **b** First differences, ΔT, showing mean, m and upper and lower 2σ values (dashed lines). **e** Calculated eccentricity of the earth's orbit. **o** calculated obliquity of the earth in its orbit. **p** Calculated precession angle of the earth in its orbit. Vertical lines in **e**, **o** and **p** show the times at which ΔT exceeds $m + 2\sigma$.

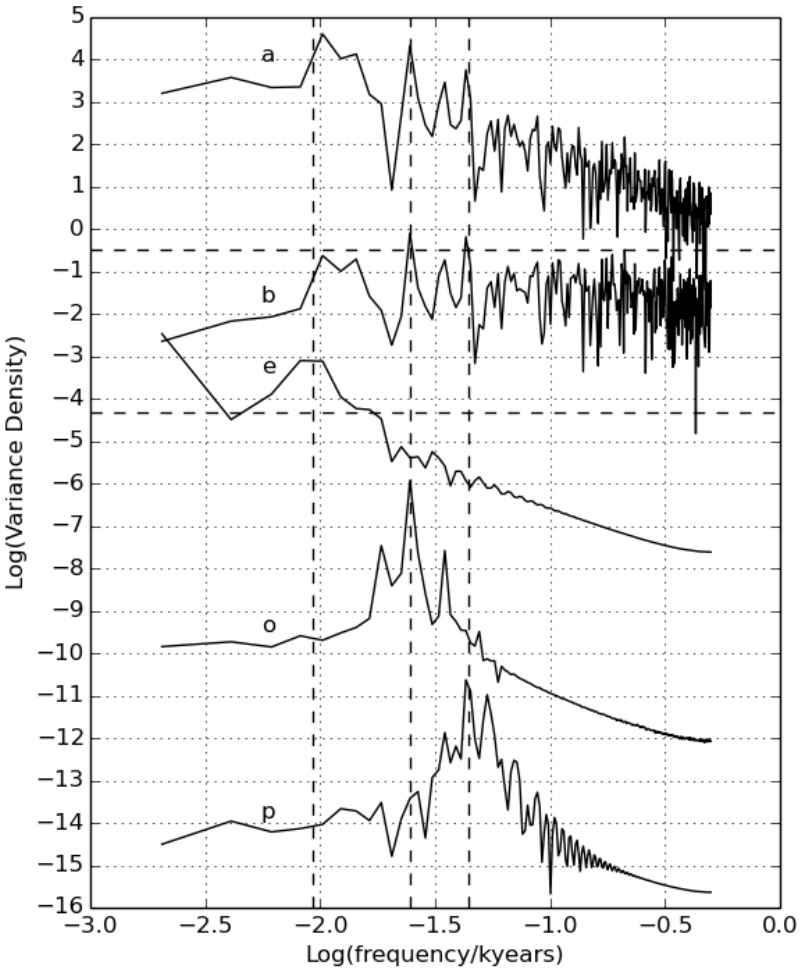

Figure 2: Periodogram spectra of the five time series depicted in Figure 1: **a** 1 kyr averaged temperatures, T, **b** First differences, ΔT, **e** eccentricity, **o** obliquity, **p** precession. Vertical dashed lines show the frequencies of the major peaks in the orbital parameter spectra at .00922, .0246 and .044 kyr^{-1} respectively. Horizontal dashed lines show the upper and lower 99.9% confidence limits of the ΔT spectrum.

the solar radiation absorbed which is proportional, in turn, to the pond's current area. Small melt ponds will thus grow exponentially until they join up to form lakes and, conceivably, lakes of continental scale. Ultimately a final ice dam will be broken and the lake's contents will pour into the ocean carrying the remaining ice with it and leaving bare earth behind.

This is the ideal case. It may not always happen like this. Firstly ponds of sufficient depth must form: ponds that are too shallow will lose all their heat by conduction during the winter. In steep terrain, underwater rivers or 'moulins' can form and drain a pond so that any stored heat finishes up in the ocean, so breaking the positive feedback cycle. There is a random component in whether melt ponds will start in the first place, whether any will deepen sufficiently to retain their heat through the first few winters and whether any will develop to be large enough for their collapse to have global consequences.

Here then is a mechanism which accounts for rapid ice age terminations:

- It accounts for storage from summer to summer,
- It has a positive feedback component whereby the area of a melt pond increases exponentially, i.e. at a rate proportional to its current area, and
- There is random component controlling whether sufficient melt ponds will form in the first place.

Water surface absorption

Another feature of melt ponds which makes them relevant to ice sheet collapse is their low albedo compared with surrounding ice and snow, see, for example, Flocco et al. (2016).

When light from a point source shines on a reflective surface at the boundary of two transparent media, part is reflected and part refracted according to Snell's Law, viz.:

$$n_1 sin(\theta_1) = n_2 sin(\theta_2) \tag{1}$$

where θ_1 and θ_2 are the angles of incidence and refraction respectively.

The amplitude of the transmitted rays depend solely on the refractive indices of the two media, n_1 and n_2. The Fresnel reflection coefficient for p-polarized and s-polarized light, r_{12p} and r_{12s}, are given by

$$r_{12p} = \frac{tan(\theta_1 - \theta_2)}{tan(\theta_1 + \theta_2)} \tag{2}$$

$$r_{12s} = \frac{sin(\theta_1 - \theta_2)}{sin(\theta_1 + \theta_2)} \tag{3}$$

The fraction of incident power reflected, R, is given by

$$R = r_{12p}^2 + r_{12s}^2 \tag{4}$$

This is, in effect, the albedo of a water surface. For most solar elevation angles it will be less than for the surrounding ice and snow. The fraction of the radiance transmitted and ultimately absorbed is $A = 1 - R$. The solar irradiance per unit horizontal area is $A(h).sin(h)$ (where $h = \pi/2 - \theta_1$ is the solar elevation angle). This can be integrated over time to give the water surface absorbed insolation. A more rigorous discussion of this topic is given by Malinka et al. (2017).

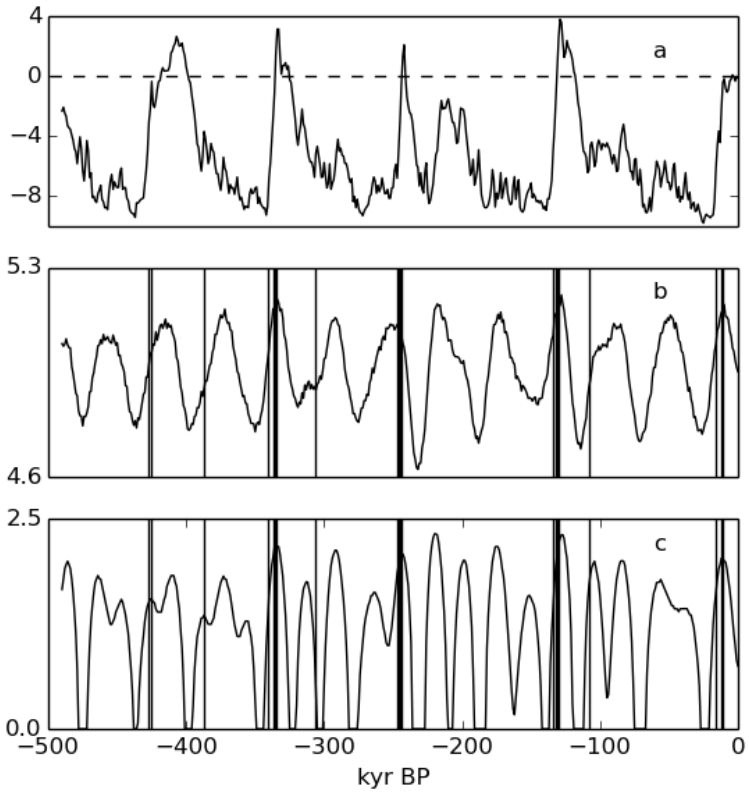

Figure 3: **a** Time series of 1 kyr averaged temperatures. **b** Annual insolation at 65° N with threshold $\tau = 275W/m^2$ (Huybers, 2006). **c** Annual water surface absorbed insolation at 65° N with threshold, $\tau = 470W/m^2$. Vertical bars show times when ΔT exceeded $m + 2\sigma$.

The *MATLAB* programs of Huybers and Eisenman (2006) for calculating daily and yearly insolation were modified to calculate daily water surface absorption of solar radiation by multiplying the irradiance at a given time and latitude by the function $A(h)$ prior to integrating. Their algorithm for rejecting those days in which the total daily insolation fell below a particular threshold, τ, was retained. The quantity calculated in this way is the water surface absorbed insolation, which was summed over the year to give annual water surface absorbed insolation (AWSAI) in units of J.m^{-2}.

Time series of AWSAI were computed for a number of high northern latitudes and threshold values, τ. These AWSAI time series were not very different from the corresponding insolation time series of Huybers for the same latitudes and thresholds; evidently the shape of the A(h) curve is not particularly important. However, the resulting time series were strongly dependent on the value of the threshold, τ, chosen. Huybers chose a value of $270W/m^2$ below which air temperature would be below the freezing point of water and no ablation of ice could be expected. The threshold value chosen here, $470W/m^2$, is almost double that. This higher threshold is justified by the fact that precipitation must be in the form of rain so that ponds can form on the ice in the first place and then not freeze overnight in the summer.

Figure 3c shows the time series for an optimum combination of latitude (65°N) and threshold ($\tau = 470W/m^2$). Time series of 1 kyr averaged temperatures and Huybers (2006) insolation time series are also shown for comparison in Figure 3a and Figure 3b, respectively. As before, vertical dashed lines indicate times when ΔT exceded $m + 2\sigma$.

Visual examination of Figure 3 shows that AWSAI is generally a better fit to the temperature time series than is insolation alone, particularly near the problematic interstadial at ∼250 kyr BP.

More detailed plots of temperature for 60 kyr during and following each of the last five Ice Age Terminations are shown in Figure 4. The temperatures plotted are the raw data from the EPICA Dome C ice cores. Rescaled plots of AWSAI are also shown as a series of lobes when the AWSAI was above the 470 W/m^2 threshold (dashed curves).

These plots show some interesting features, viz.:

1. Termination temperature peaks were 1 to 3 kyr wide and followed by a plateau in temperature such as the Holocene.

2. In each case the temperature peaked near the time of maximum AWSAI of the Termination Lobe.

3. Following Terminations I to IV, in each case temperature began to fall more rapidly after the end of the Termination Lobe.

4. Following Terminations I to IV, in each case temperature fell by about 5°C between the end of the Termination Lobe and the beginning of the subsequent lobe.

Melt ponds and ice sheet dynamics

The first part of this chapter is based on a paper submitted to a peer-reviewed journal. The paper was rejected on the advice of the Associate Editor who reasoned as follows:

1. *Less than half of melt ponds in Greenland store water between seasons with the remainder emptying by either vertical or lateral drainage (Selmes et al., 2013).*

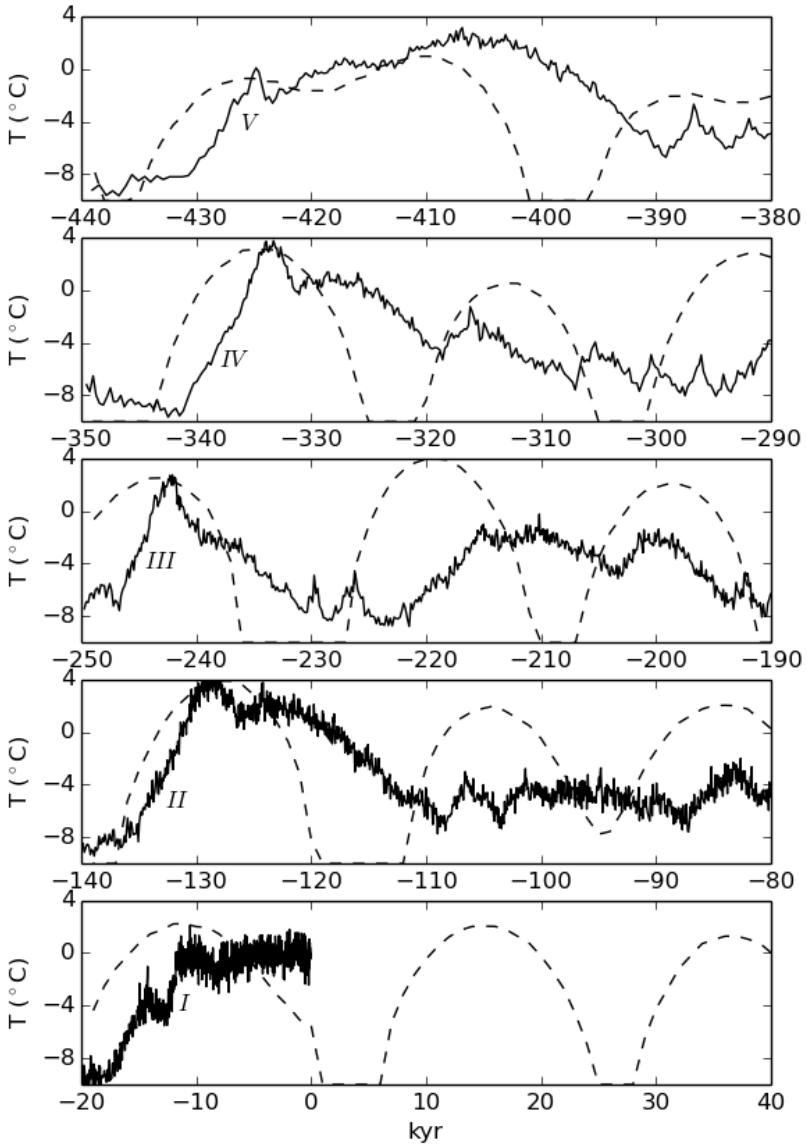

Figure 4: Epica Dome C Ice Core Deuterium temperature estimates (solid line) and annual water surface absorbed insolation at 65° N (dashed line) for the intervals including and following the five last Ice Age Terminations (V, IV, III, II and I).

2. *Melt ponds on grounded ice do not form randomly. Their location and size is controlled by the topographic depressions in which they form. These depressions, in turn, are controlled by the topography of the underlying bedrock (Echelmeyer et al., 1991).*

3. *Since ice flows, any ice which has been subject to enhanced ablation due to the presence of the melt-pond is advected downstream. On Greenland, the ice on which a lake sits is renewed approximately every 10 years. This, together with (2) means that it is impossible for exponential lake growth to occur through enhanced ablation on grounded ice.*

This view, that the ice sheet dynamics of present day Greenland provides a suitable model for the behaviour of the Ice Sheets during the last five Terminations, is not justified; they are very different scenarios. In present day Greenland, large outlet glaciers, which are restricted tongues of the ice sheet, move through bordering valleys around the periphery of Greenland to calve off into the ocean. The best known of these outlet glaciers is the Jakobshavn Glacier discussed by Echelmeyer et al., which, at its terminus, flows at speeds of 7000 m/yr. A comprehensive study of ice streams by Margold et al. (2015) has shown that flow speeds over most of the area of the Laurentide Ice Sheet were close to zero at the time of the Last Glacial Maximum (Margold et al., Figure 2). Given the accepted dynamics of ice flow, these regions must have been almost flat and horizontal in contrast to the steep Greenland ice flows.

Furthermore, the present day is a time of decreasing solar declination and water surface absorption. In contrast, Terminations occurred at times of increasing solar declination when old, static, horizontal ice was increasingly exposed to solar radiation, so allowing new melt ponds to form when rain fell during the summer months.

Conclusions

The catastrophic collapse of ice sheet melt lakes appears to have first been proposed by Bretz (1923) who attributed the scouring of the Scablands of Washington State to the draining of Lake Missoula in western Montana. Since then many other topographic features have been seen to be associated with such dramatic collapses, see, for example, Patton et al. (2017).

That melt ponds and melt lakes play a major role in amplifying the effects of increased Northern Hemisphere insolation has hitherto gone unnoticed. These catastrophic climate disruptions are surely the most important feature of the Late Pleistocene and, in a sense, define it.

The succession of Ice Ages and Interglacials, of Stadials and Interstadials, is a deterministically forced stochastic process, very much like present-day weather but at longer time scales. There is little evidence of other deterministic cycles forcing climate between the annual cycle and the precession cycle, i.e. between one year and 23,000 years in period: a span of four orders of magnitude. Supposed "multidecadal cycles" are nothing more than red noise.

According to Figure 4, under this model, on a time scale of millennia, the next Ice Age has already commenced. The present "Holocene" lobe of AWSAI comes to an end in 1200 years time, and the subsequent lobe commences 5000 years after that. Based on previous interglacials, we can speculate that global average temperature is likely to be 5°C cooler in 6000 years time.

Software

The *Python* programs used to generate the diagrams found in this chapter, *OPspectra.py, OPlist.py* and *DailyInsolation.py*, are listed below. The relevant data files can be downloaded from `http://blackjay.net/?page_id=892`.

OPspectra.py

```
""" OPspectra.py - reads temperature, eccentricity, epsilon and
    omega for the last 490 kyear listed in OP491 prepared by
    opList.py. Plots time series and spectra of T, dT, ecc,
    epsilon and omega.
    Shows times when dT exceeds 2 standard deviations from the mean.
    Shows 99.9 percent confidence limits for dT spectrum.
"""
import numpy as np
import matplotlib.pyplot as plt
from matplotlib import gridspec
from scipy.fftpack import fft, ifft
from scipy import stats
#
ipfile='OP491'
Ns = len(open(ipfile).readlines())-1
print 'Ns = ',Ns
f = open(ipfile, 'r')

kyear = np.zeros(Ns,float)
kym = np.zeros(Ns-1,float)
T = np.zeros(Ns,float)
dT = np.zeros(Ns-1,float)
ecc = np.zeros(Ns,float)
epsilon = np.zeros(Ns,float)
omega = np.zeros(Ns,float)
i = 0
j = 0
for line in f:
        if i>0:
                myline = line.split()
                kyear[j] = -float(myline[0])
                T[j] = float(myline[1])
                ecc[j] = float(myline[2])
                epsilon[j] = float(myline[3])
                omega[j] = float(myline[4])
                j+=1
        i+=1
f.close()
prec=np.sin(omega)

for i in range(Ns-1):
        dT[i]=T[i]-T[i+1]
        kym[i]=.5*(kyear[i]+kyear[i+1])

#
figname=ipfile
#
#
fig=plt.figure(num=1,figsize=(6.4,9.6))
gs = gridspec.GridSpec(5, 1, height_ratios=[1,1,1,1,1])
#
ax=plt.subplot(gs[0])
plt.plot(kyear,T,color='k')
#plt.title(figname)
plt.ylim(-10.0,4.0)
plt.yticks([-8,-4,0,4])
plt.xlim(-500,0)
plt.xticks([])
plt.hlines(0,-499,0,linestyle='--')
ax.annotate('a',xy=(.95,.1),xycoords='axes fraction',\
```

```
xytext=(.92,.8), textcoords='axes fraction')

ax=plt.subplot(gs[1])
plt.plot(kym,dT,color='k')
plt.xlim(-500,0)
plt.xticks([])
plt.ylim(-3,3)
plt.yticks([-3,0,3])
mean=np.mean(dT)
std=np.std(dT)
plt.hlines(mean+2*std,-499,0,linestyle='--')
plt.hlines(mean,-499,0,linestyle='--')
plt.hlines(mean-2*std,-499,0,linestyle='--')
ax.annotate('b',xy=(.95,.1),xycoords='axes fraction',\
xytext=(.92,.8), textcoords='axes fraction')

ax=plt.subplot(gs[2])
plt.plot(kyear,ecc,color='k')
plt.ylim(0,.05)
plt.xlim(-500,0)
plt.xticks([])
plt.yticks([0,.05])
for i in range(Ns-2):
        if dT[i]>mean+2*std:
                plt.vlines(kym[i],0,.05)
ax.annotate('e',xy=(.95,.1),xycoords='axes fraction',\
xytext=(.92,.8), textcoords='axes fraction')

ax=plt.subplot(gs[3])
plt.plot(kyear,epsilon,color='k')
plt.xlim(-500,0)
plt.xticks([])
plt.ylim(.38,.43)
plt.yticks([.38,.43])
for i in range(Ns-2):
        if dT[i]>mean+2*std:
                plt.vlines(kym[i],.38,.43)
ax.annotate('o',xy=(.95,.1),xycoords='axes fraction',\
xytext=(.92,.8), textcoords='axes fraction')

ax=plt.subplot(gs[4])
plt.plot(kyear,prec,color='k')
plt.ylim(-1,1)
plt.xlim(-500,0)
plt.xlabel('kyr BP')
plt.yticks([-1,0,1])
plt.hlines(0,-499,0,linestyle='--')
for i in range(Ns-2):
        if dT[i]>mean+2*std:
                plt.vlines(kym[i],-1,1)
ax.annotate('p',xy=(.95,.1),xycoords='axes fraction',\
xytext=(.9,.8), textcoords='axes fraction')

plt.savefig(figname)
plt.show()
#
#        Normalize all time series to zero mean and unit variance
#
T=(T-np.mean(T))/np.std(T)
dT=(dT-np.mean(dT))/np.std(dT)
#
figname="OPspectra"
```

```
f=open('OPPgrams','w')
fig=plt.figure(num=1,figsize=(6.4,8.0))
gs = gridspec.GridSpec(1, 1, height_ratios=[1])
ax=plt.subplot(gs[0])
#
X = np.linspace(0,0.5,(Ns)/2)
XX = X[1:]
lX = np.log(XX)/np.log(10.)
#
Y = fft(T)
S = np.abs(Y[0:(Ns)/2])**2
SS = S[1:]
lS = np.log(SS)/np.log(10.)
plt.plot(lX,lS,color='k')
ax.annotate('a',xy=(.95,.1),xycoords='axes fraction',\
xytext=(.25,.95), textcoords='axes fraction')
f.write('\n a    log f    log P        P        f        T   \n')
for i in range(31):
        f.write(\
        '{0:2d} {1:8.3f} {2:8.3f} {3:8.0f} {4:8.5f} {5:8.4f}\n'.\
        format(i,lX[i],lS[i],SS[i],XX[i],1/XX[i]))
#
Y = fft(dT)
S = np.abs(Y[0:(Ns)/2])**2
SS = S[1:]
lS = np.log(SS)/np.log(10.)
plt.plot(lX,lS-4,color='k')
#
#        Prepare confidence limits using F-test
#
Sbar=np.mean(S)
lSbar=np.log(Sbar)/np.log(10.)
dfn = 2
dfd = Ns-1
cl001 = np.log(Sbar*stats.f.ppf(.001,dfn,dfd))/np.log(10.)
cl999 = np.log(Sbar*stats.f.ppf(.999,dfn,dfd))/np.log(10.)
plt.hlines(cl999-4,-3.,0.,color='k',linestyle='--')
plt.hlines(cl001-4,-3.,0.,color='k',linestyle='--')
ax.annotate('b',xy=(.7,.1),xycoords='axes fraction',\
xytext=(.25,.68), textcoords='axes fraction')
f.write('\n b    log f    log P        P        f        T   \n')
for i in range(31):
        f.write(\
        '{0:2d} {1:8.3f} {2:8.3f} {3:8.0f} {4:8.5f} {5:8.4f}\n'.\
        format(i,lX[i],lS[i],SS[i],XX[i],1/XX[i]))
#
Y = fft(ecc)
S = np.abs(Y[0:(Ns)/2])**2
SS = S[1:]
lS = np.log(SS)/np.log(10.)
plt.plot(lX,lS-3.5,color='k')
ax.annotate('e',xy=(.95,.1),xycoords='axes fraction',\
xytext=(.25,.6), textcoords='axes fraction')
f.write('\n c    log f    log P        P        f        T   \n')
for i in range(31):
        f.write(\
        '{0:2d} {1:8.3f} {2:8.3f} {3:8.0f} {4:8.5f} {5:8.4f}\n'.\
        format(i,lX[i],lS[i],SS[i]*10000,XX[i],1/XX[i]))
#
Y = fft(epsilon)
S = np.abs(Y[0:(Ns)/2])**2
SS = S[1:]
```

```
lS = np.log(SS)/np.log(10.)
plt.plot(lX,lS-7.1,color='k')
ax.annotate('o',xy=(.95,.1),xycoords='axes fraction',\
xytext=(.25,.31), textcoords='axes fraction')
f.write('\n d    log f    log P        P        f        T   \n')
for i in range(31):
        f.write(\
        '{0:2d} {1:8.3f} {2:8.3f} {3:8.0f} {4:8.5f} {5:8.4f}\n'.\
        format(i,lX[i],lS[i],SS[i]*10000,XX[i],1/XX[i]))
#
Y = fft(prec)
S = np.abs(Y[0:(Ns)/2])**2
SS = S[1:]
lS = np.log(SS)/np.log(10.)
plt.plot(lX,lS-15,color='k')
ax.annotate('p',xy=(.95,.1),xycoords='axes fraction',\
xytext=(.25,.1), textcoords='axes fraction')
f.write('\n e    log f    log P        P        f        T   \n')
for i in range(31):
        f.write(\
        '{0:2d} {1:8.3f} {2:8.3f} {3:8.0f} {4:8.5f} {5:8.4f}\n'.\
        format(i,lX[i],lS[i],SS[i]*1000,XX[i],1/XX[i]))
#
f.close()
plt.ylim(-16,5)
plt.yticks([-16,-15,-14,-13,-12,-11,-10,-9,-8,-7,-6,-5,-4,\
-3,-2,-1,0,1,2,3,4,5])
plt.grid()
plt.xlabel("Log(frequency/kyears)")
plt.ylabel("Log(Variance Density)")
#
#        Plot key frequencies.
#
keyf=np.array([.00922,.0246,.044])
lkeyf=np.log(keyf)/np.log(10.)
for lkeyf1 in lkeyf:
        plt.vlines(lkeyf1,-16,5,color='k', linestyle='--')
#
plt.savefig(figname)
plt.show()
```

OPlist.py

```
""" OPlist - writes list of orbital parameters vs kyear
        Data files, DomeCdeuterium.txt and orbital_parameter_data.mat
        can be downloaded from http://blackjay.net/?page_id=892
"""
import numpy as np
import scipy.io as spio
import matplotlib.pyplot as plt
from matplotlib import gridspec
import DailyInsolation as DI
#
#
#
#         Dome C deuterium
#
#   read in raw data
#
Nr = 5159
f = open('DomeCdeuterium.txt', 'r')
title = 'EPICA Dome C Deuterium'
rx = np.zeros(Nr,float)
ry = np.zeros(Nr,float)
i = 1
j = 0
for line in f:
    if i>104:
        myline = line.split()
        #print myline, len(myline)
        if len(myline)>4:
            rx[j] = float(myline[2])/1000.
            ry[j] = float(myline[4])
            if rx[j]>490:
                break
            j+=1
    i+=1
f.close()
#
#   prepare time series
#
tmin = 0
#tmax=5
tmax = 491.
#Ns = 5
Ns = 491
dt = (tmax-tmin)/Ns
df = 1/(Ns*dt)
fN= 0.5/dt              #Nyquist frequency
x = np.zeros(Ns,float)
y = np.zeros(Ns,float)
Nempty = 0
for j in range(Ns):
    x[j] = tmin+j*dt
    t1 = tmin+j*dt-dt/2
    t2 = tmin+j*dt+dt/2
    nj = 0
    sj = 0
    for i in range(Nr):
        if t1<rx[i] and rx[i]<=t2:
            nj+=1
            sj+=ry[i]
    if nj>0:
```

```
        y[j]=sj/nj
    else:
        if j>0:
            y[j]=y[j-1]
            Nempty += 1
        else:
            y[0]=ry[0]
        print "no data in <",t1,",",t2,">"
print Nempty, " empty intervals."
#print x
#
#
#
kyear=-x.copy()
ecc,epsilon,omega=DI.orbital_parameters(-kyear)
opfile='OP{0:03d}'.format(Ns)
f=open(opfile,'w')
header='kyr          T        ecc    epsilon        omega\n'
f.write(header)
for iy,kyear1 in enumerate(kyear):
        string='{0:3.0f} {1:10.6f} {2:10.6f} {3:10.6f} {4:12.6f}\n'\
.format(-kyear1,y[iy],ecc[iy],epsilon[iy],omega[iy])
        f.write(string)
f.close()
```

DailyInsolation.py

```
""" DailyInsolation.py - Functions for computing Daily Insolation.

        Data files, DomeCdeuterium.txt and orbital_parameter_data.mat
        can be downloaded from http://blackjay.net/?page_id=892

 References:
   Berger A. and Loutre M.F. (1991). Insolation values for the
   climate of the last 10 million years.
   Quaternary Science Reviews, 10(4), 297-317.
   Berger A. (1978). Long-term variations of daily insolation and
   Quaternary climatic changes.
   Journal of Atmospheric Science, 35(12), 2362-2367.

 Authors:
 MATLAB
   Ian Eisenman and Peter Huybers, Harvard University, August 2006
   eisenman@fas.harvard.edu
   This file is available online at
   http://deas.harvard.edu/~eisenman/downloads
 PYTHON
   John Reid
   johnsinclairreid@gmail.com
"""
import numpy as np
import scipy.io as spio

def daily_insolation(*args):
        kyear=args[0]
        lat=args[1]
        day=args[2]
        n1=1.                #refractive index of air
        n2=1.333        #refractive index of Water
        tiny=1.4e-45
        [ecc,epsilon,omega]=orbital_parameters(-kyear)
        obliquity=epsilon*180/np.pi
        long_perh=omega*180/np.pi
        lat=lat*np.pi/180         # latitude
        delta_lambda_m=(day-80)*2*np.pi/365.2422
        beta=(1-ecc**2)**(1/2)
        lambda_m0=-2*((1/2*ecc+1/8*ecc**3)*(1+beta)*np.sin(-omega)\
        -1/4*ecc**2*(1/2+beta)*np.sin(-2*omega)\
        +1/8*ecc**3*(1/3+beta)*(np.sin(-3*omega)))
        lambda_m=lambda_m0+delta_lambda_m
        lambda1=lambda_m+(2*ecc-1/4*ecc**3)*np.sin(lambda_m-omega)
        lambda1+=(5/4)*ecc**2*np.sin(2*(lambda_m-omega))
        lambda1+=(13/12)*ecc**3*np.sin(3*(lambda_m-omega))
        So=1365
        # solar constant (W/m**2)
        delta=np.arcsin(np.sin(epsilon)*np.sin(lambda1))
        # declination of the sun
        cnst=So/np.pi*(1+ecc*np.cos(lambda1-omega))**2/(1-ecc**2)**2
        Ho=np.empty_like(delta)
        Fsum=np.empty_like(delta)
        Asum=np.empty_like(delta)
        for index,delta1 in np.ndenumerate(delta):
                if(abs(lat)>=np.pi/2-abs(delta1)) and (lat*delta1>0):
                        Ho[index]=np.pi
                elif(abs(lat)>=np.pi/2-abs(delta1)) \
                and (lat*delta1 <= 0):
                        Ho[index]=0
```

```
                else:
                        Ho[index]=np.arccos(-np.tan(lat)\
                        *np.tan(delta1))        \
                        #hour angle at sunrise/set
                num=20
                dh=Ho[index]/num
                Fsum[index]=0
                Asum[index]=0
                for h in np.linspace(0,Ho[index],num):
                        sinh=(np.sin(lat)*np.sin(delta1)\
                         + np.cos(lat)*np.cos(delta1)*np.cos(h))*dh
                        Fsum[index]+=sinh
                        theta1 = np.pi/2-h
                        theta2 = np.arcsin(n1*np.sin(theta1)/n2)
                        plus=theta1+theta2
                        if abs(plus)<tiny:
                                plus=tiny
                        minus=theta1-theta2
                        if abs(minus)<tiny:
                                minus=tiny
                        r12p=np.tan(minus)/np.tan(plus)
                        r12s=np.sin(minus)/np.sin(plus)
                        FracReflected=0.5*(r12p**2+r12s**2)
                        FracAbsorbed = 1.0-FracReflected
                        Asum[index]+=sinh*FracAbsorbed
        Fsw=cnst*(Ho*np.sin(lat)*np.sin(delta) \
        + np.cos(lat)*np.cos(delta)*np.sin(Ho))
        Ftest=cnst*Fsum
        WSAbs=cnst*Asum
        return Fsw, ecc, obliquity, long_perh, Ftest, WSAbs

def orbital_parameters(year):
        tmax=5001                       # max years before present
        mat = spio.loadmat('orbital_parameter_data.mat'\
        ,squeeze_me=True)
        m=np.array(mat['m'])
        kyear0=m[:tmax,0]
        # kyears before present for data (kyear0>=0)
        ecc0=m[:tmax,1]                 # eccentricity
        # add 180 degrees to omega
        #(see lambda definition, Berger 1978 Appendix)
        omega0=m[:tmax,2]+180
        # longitude of perihelion (precession angle)
        omega0=np.unwrap(omega0*np.pi/180)*180/np.pi\
# remove discontinuities (360 degree jumps)
        epsilon0=m[:tmax,3]         # obliquity angle
        iyear=year.astype(int)
        frac=year-iyear
        ecc=ecc0[iyear]+frac*(ecc0[iyear+1]-ecc0[iyear])
        omega=(omega0[iyear]+frac*(omega0[iyear+1]\
        -omega0[iyear]))*np.pi/180
        epsilon=(epsilon0[iyear]+frac*(epsilon0[iyear+1]\
        -epsilon0[iyear]))*np.pi/180
        return ecc,epsilon,omega
```

References

Berger, A. L. (1979). Long-term variations of daily insolation and quaternary climatic changes. *Journal of the Atmospheric Sciences 35*, 2362–2367.

Berger, A. L. and M. F. Loutre (1991). Insolation values for the climate of the last 10 million years. *Quaternary Science Reviews 10*(4), 297–317.

Bretz, J. H. (1923). The channeled scabland of the columbia plateau. *Journal of Geology 31*, 617–649.

Echelmeyer, K., T. Clarke, and W. Harrison (1991). Surficial glaciology of jakobshavns isbræ, west greenland: Part i. surface morphology. *Journal of Glaciology 37*(127), 368–382.

Flocco, D., D. L. Feltham, D. Schroeder, and M. Tsamados (2016). Impact of refreezing melt ponds on arctic sea ice basal growth. *The Cryosphere Discuss.*.

Hays, J. D., J. Imbrie, and N. J. Shackleton (1976). Variations in the earth's orbit: Pacemaker of the ice ages. *Science 194*(4270), 1121–1132.

Huybers, P. (2006). Early pleistocene glacial cycles and the integrated summer insolation forcing. *Science 313*(5786), 508–511.

Huybers, P. and I. Eisenman (2006). Integrated summer insolation calculations. *IGBP PAGES/World Data Center for Paleoclimatology, Data Contribution Series 2006-079. NOAA/NCDC Paleoclimatology Program, Boulder CO, USA*.

Jouzel, J., V. Masson-Delmotte, O. Cattani, G. Dreyfus, S. Falourd, G. Hoffmann, B. Minster, J. Nouet, J. Barnola, J. Chappellaz, H. Fischer, J. Gallet, S. Johnsen, M. Leuenberger, L. Loulergue, D. Luethi, H. Oerter, F. Parrenin, G. Raisbeck, D. Raynaud, A. Schilt, J. Schwander, E. Selmo, R. Souchez, R. Spahni, B. Stauffer, J. P. Steffensen, B. Stenni, T. F. Stocker, J. L. Tison, M. Werner, and E. W. Wolff (2007). Orbital and millennial antarctic climate variability over the past 800,000 years. *Science 317*(5839), 793–797.

Malinka, A., E. Zege, L. Istomena, G. Heygster, G. Spreen, D. Perovich, and C. Polashenski (2017). Reflective properties of melt ponds on sea ice. *The Cryosphere Discuss.*.

Margold, M., C. R. Stokes, and C. D. Clark (2015). Ice streams in the laurentide ice sheet:f identification, characteristics and comparison to modern ice sheets. *Earth Science Reviews 143*, 117–146.

Maslin, M. and A. Ridgwell (2005). Mid-pleistocene revolution and the "eccentricity myth". *Geological Society, London, Special Publications 247*, 19–34.

Milankovitch, M. (1941). *K. Serb. Akad. Beogr. Spec. Publ. 132*.

Patton, H., A. H. A., K. Andreassen, A. Auriac, P. L. Whitehouse, A. P. Stroevenc, C. Shackleton, M. Winsborrow, J. Heyman, and A. M. Hall (2017). Deglaciation of the eurasian ice sheet complex. *Quaternary Science Reviews 169*, 148–172.

Reid, J. (2019). *The Fluid Catastrophe*, pp. 31–86. Newcastle upon Tyne: Cambridge Scholars Publishing.

Selmes, N., T. Murray, and T. D. James (2013, February). Characterizing supraglacial lake drainage and freezing on the Greenland Ice Sheet. *The Cryosphere Discussions 7*, 475–505.

Bibtex Citation

```
@inbook{ReidIA,
        AUTHOR = {Reid, John},
        YEAR = {2019},
        TITLE = {The Fluid Catastrophe},
        PUBLISHER = {Cambridge Scholars Publishing},
        ADDRESS = {Newcastle upon Tyne},
        ISBN = {1-5275-3206-2},
        CHAPTER = {11},
        pages = {89-103}
}
```